

# The Hughes model for pedestrian dynamics and congestion modelling<sup>\*</sup>

Elisabetta Carlini<sup>\*</sup> Adriano Festa<sup>\*\*</sup> Francisco J. Silva<sup>\*\*\*</sup>

<sup>\*</sup> *Dipartimento di Matematica “G. Castelnuovo”, Sapienza Università di Roma, (e-mail: carlini@mat.uniroma1.it).*

<sup>\*\*</sup> *RICAM – Johann Radon Institute for Computational and Applied Mathematics (ÖAW), (e-mail: adriano.festa@oaw.ac.at)*

<sup>\*\*\*</sup> *XLIM - DMI UMR CNRS 7252 Faculté des Sciences et Techniques, Université de Limoges, (e-mail: francisco.silva@unilim.fr)*

---

**Abstract:** In this paper we present a numerical study of some variations of the Hughes model for pedestrian flow under different types of congestion effects. The general model consists of a coupled non-linear PDE system involving an eikonal equation and a first order conservation law, and it intends to approximate the flow of a large pedestrian group aiming to reach a target as fast as possible, while taking into account the congestion of the crowd.

We propose an efficient semi-Lagrangian scheme (SL) to approximate the solution of the PDE system and we investigate the macroscopic effects of different penalization functions modelling the congestion phenomena.

*Keywords:* Partial differential equations, social and behavioral sciences, dynamic modelling, numerical simulations, characteristic curves.

---

## 1. INTRODUCTION

In the last years the understanding of the dynamics underneath the pedestrian crowd motion has attracted a wide attention in public debate and in the scientific community. The complete comprehension of such phenomena remains still as a subject of active research. Nevertheless, important progresses have been made in the past two decades and several mathematical models have been proposed for its description.

The different approaches to tackle the problem can be classified according to the scale of the model: they range from microscopic systems, where each trajectory is described individually, to macroscopic systems, where the dynamics of the crowd is modelled as a time-evolving density distribution of indistinguishable agents. For a detailed overview we refer e.g. to the work by Bellomo and Dogbe (2011) and the monograph by Cristiani et al. (2014).

In the article by Hughes (2000), the author introduced a by now classical fluid-dynamical model to study the motion of a large human crowd. The crowd is treated as a “thinking fluid” and it moves at maximum speed towards a common target, while taking into account environmental factors such as the congestion of the crowd. In this model people prefer to avoid crowded regions and this assumption is incorporated in a potential function which determines the velocity field driving the crowd. Indeed, the potential is

characterized as the gradient of the solution of an eikonal equation with a right hand side which depends on the current distribution of the crowd. Hence, given a time horizon  $T > 0$ , for each time instant  $t \in [0, T]$ , each microscopical individual looks at the global configuration of the crowd and updates his/her velocity trying to avoid the current crowded regions.

In a two-dimensional space setting, given  $f : [0, +\infty[ \rightarrow \mathbb{R}$ , a bounded domain  $\Omega \in \mathbb{R}^2$  and a target  $\mathcal{T} \subseteq \Omega$ , the model is given by

$$\begin{cases} \partial_t m(x, t) - \operatorname{div}(f^2(m(x, t)) \nabla u(x, t) m(x, t)) = 0, & \text{in } \Omega \times ]0, T[, \\ |\nabla u(x, t)| = \frac{1}{f(m(x, t))}, & \text{in } (\Omega \setminus \mathcal{T}) \times ]0, T[, \end{cases} \quad (1)$$

complemented with the boundary conditions

$$\begin{cases} m(x, 0) = m_0(t), & \text{on } \Omega \times \{0\}, \\ u(x, t) = 0, & \text{on } \mathcal{T} \times (0, T), \\ u(x, t) = g(x) & \text{on } \partial\Omega \times (0, T), \\ (f^2(m) \nabla u m)(x, t) \cdot \hat{n}(x) = 0, & \text{on } \partial\Omega \times (0, T). \end{cases} \quad (2)$$

In (1) the gradient operator  $\nabla$  acts on the space variable  $x$ , the unknown variable  $m$  is the pedestrian density and  $u$  is the potential, i.e. the weighted shortest distance to the target  $\mathcal{T}$ . Concerning the boundary conditions (2), we assume that  $g$  is a continuous function large enough to satisfy some compatibility conditions, see e.g. (Bardi and Dolcetta, 1996, Chapter IV), and  $\hat{n}$  denotes the outward normal to the boundary  $\partial\Omega$ . System (1) is a highly non-linear coupled system of PDEs. Few analytic results are available, all of them restricted to spatial dimension one and particular choices for the function  $f$  (see the works by Di Francesco et al. (2011) and Amadori et al. (2014)).

---

<sup>\*</sup> EC acknowledges financial support from INDAM GnCS, project “Metodi numerici semi-impliciti e semi-Lagrangiani per sistemi iperbolici di leggi di bilancio”. AF acknowledge financial support from the Austrian Academy of Sciences ÖAW via the New Frontiers Group NST-001. FJS benefited from the support of the “FMJH Program Gaspard Monge in optimization and operation research”, and from the support to this program from EDF.

The main difficulty comes from the low regularity of the potential  $u$ , which is only Lipschitz-continuous.

Hughes proposed a few functions  $f$ 's penalizing regions of high density, the simplest choice being  $f(m) = 1 - m$  where 1 corresponds to the maximum scaled pedestrian density. In this work we focus our attention on numerical methods to solve (1)-(2) for several choices of the penalty function  $f$ . We must underline that since well-posedness results for (1)-(2) have not been proved in full generality yet, convergence results of numerical algorithms for (1)-(2) seem currently out of reach. Thus, we will consider some heuristics to solve (1)-(2) based on recent techniques introduced in Carlini and Silva (2014), Carlini and Silva (2015) and Carlini et al. (2016). We point out that the article by Carlini et al. (2016) concerns the approximation of a regularized version of (1)-(2). Our strategy is to look at (1)-(2) as a single non-linear continuity equation, which can be approximated by discretizing the characteristics governing the equation with an Euler scheme. However, the velocity field describing the characteristics depends at each time step non-locally on the current distribution of the agents and has to be computed with the help of the eikonal equation, for which several efficient methods exist.

## 2. A SEMI-LAGRANGIAN SCHEME FOR THE APPROXIMATION OF THE SYSTEM

### 2.1 Modeling aspects

As in the theory of Mean Field Games (MFGs), system (1) can, *at least formally*, be interpreted as a sort of Nash equilibrium for a dynamical game involving a continuous number of agents. Indeed, given a space-time distribution density of the agents  $(x, t) \in \Omega \times [0, T] \mapsto m(x, t) \in \mathbb{R}$ , such that  $m \geq 0$ , the solution  $u[m]$  of the second equation in (1) can be formally represented as the value function of the *optimal control problem*

$$u[m](x, t) = \inf_{\alpha \in \mathcal{A}} \int_t^{\tau^{x,t}[\alpha]} F(m(X^{x,t}[\alpha](s), t)) ds, \quad (3)$$

where

$$\mathcal{A} := \{ \alpha : [0, T] \mapsto \mathbb{R}^d ; |\alpha(t)| \leq 1, \text{ a.e. in } [0, T] \},$$

$$X^{x,t}[\alpha](s) := x + \int_t^s \alpha(r) dr \quad \forall s \in [t, T],$$

$$\tau^{x,t}[\alpha] := \inf \{ s \in [t, T] ; X^{x,t}[\alpha](s) \in \mathcal{T} \},$$

$$\text{and } F(m) := \frac{1}{f(m)}.$$

Thus,  $u[m](x, t)$  corresponds to the *weighted minimal time* to reach the target set  $\mathcal{T}$  for a *typical player* positioned at  $x$  at time  $t$ . From the modelling point of view, it is fundamental to notice that in its individual cost the typical agent *freezes* the global distribution  $m$  at time  $t$  and thus s/he does not forecast the future behaviour of the population in order to determine its optimal policy. This modelling aspect shows an important difference with MFG models, where, at the equilibrium, the agents take into account the future distribution of the population in order to design their strategies.

Then, after the optimal feedback law

$$s \in [t, T] \mapsto \bar{\alpha}[t](s) := - \frac{\nabla u[m](X^{x,t}[\hat{\alpha}](s), t)}{|\nabla u[m](X^{x,t}[\hat{\alpha}](s), t)|} \quad (4)$$

is computed, the agents *actually* move according to the dynamics defined by the the solution of the ODE

$$\frac{d\hat{X}^{t,x}}{ds}(s) = - \frac{\nabla u[m](\hat{X}^{x,t}(s), s)}{|\nabla u[m](\hat{X}^{x,t}(s), s)|} f(m(\hat{X}^{t,x}(s), s)), \quad (5)$$

for  $s \in [t, T]$ . Note that at each time  $s \in [s, T]$  the agents must re-optimize their cost in terms of  $m(\cdot, s)$  since, by (5), the agents move accordingly to the feedback law

$$(x, s) \in \Omega \times [t, T] \mapsto - \frac{\nabla u[m](x, s)}{|\nabla u[m](x, s)|}$$

rather than

$$(x, s) \in \Omega \times [t, T] \mapsto - \frac{\nabla u[m](x, t)}{|\nabla u[m](x, t)|}$$

(see (4)). In addition, their desired velocity field is rescaled by  $f(m(\cdot, \cdot))$  modelling that congestion also affects *directly* the velocity of each individual agent. Based on (5) we get that the evolution  $m$  of the initial distribution leads, at least heuristically, to the non-linear continuity equation

$$\begin{aligned} \partial_t m - \operatorname{div}(f^2(m) \nabla u[m] m) &= 0, \\ m(x, 0) &= m_0(x), \end{aligned} \quad (6)$$

which is, of course, equivalent to (1)-(2) (omitting the Neumann boundary condition in (2) for  $m$ , which amounts to say that the trajectories followed by the agents are reflected at  $\partial\Omega \setminus \mathcal{T}$ ). Natural fixed point strategies to study the existence of solutions of (1) (or (6)) usually fail because of the lack of enough regularity for the solutions of both equations separately. We refer the reader to the article by Di Francesco et al. (2011) where an existence result is proved in the one-dimensional case  $d = 1$  by approximating system (1) by analogous systems involving small diffusion parameters for which the well-posedness can be shown with the help of classical arguments in PDE theory. Other existence results are described in Amadori and Di Francesco (2012); Amadori et al. (2014).

Based on the trajectorial description presented above for both equations in (1), we consider in the next section a natural discretization of (6), based on an Euler discretization of equation (5) and the fact that solutions of (6) can be interpreted as the push-forward of  $m_0$  under the flow induced by (5) (cf. Carlini and Silva (2014); Piccoli and Tosin (2011)).

### 2.2 A semi-Lagrangian scheme for a non-linear conservation law

Equation (6) shows that (1) can be interpreted as a non-linear continuity equation. Note that (3) implies that the non-linear term  $\nabla u[m]$  in (6) depends *non-locally* on  $m$ . In view of the previous remarks, let us describe now a SL scheme designed to numerically solve general non-linear continuity equations. The scheme we present here has been first proposed in Carlini and Silva (2014) and in Carlini and Silva (2015) in order to approximate first and second order MFGs, respectively. Then, an extension of the scheme, designed for a regularized version of (1), has been implemented in Carlini et al. (2016). We also refer the reader to Festa et al. (2016) where the scheme has been applied to a non-linear continuity equation modelling a kinetic pedestrian model. We recall here the scheme for the case of a two dimensional non-linear continuity equation

on a bounded domain  $\Omega$  with Neumann condition on the boundary  $\partial\Omega$ :

$$\begin{cases} \partial_t m + \operatorname{div}(b[m](x, t) m) = 0 & \text{in } \Omega \times (0, T), \\ b[m](x, t) m \cdot \hat{n} = 0 & \text{on } \partial\Omega \times (0, T), \\ m(\cdot, 0) = m_0(\cdot) & \text{in } \Omega. \end{cases} \quad (7)$$

Here,  $b[m] : \Omega \times [0, T] \rightarrow \mathbb{R}$  is a given smooth vector field, depending on  $m$ ,  $m_0$  a smooth initial datum defined on  $\Omega$  and  $\hat{n}$  the unit outer normal vector to the boundary  $\partial\Omega$ . Formally, at time  $t \in [0, T]$  the solution of (7) is given, implicitly, by the image of the measure  $m_0 dx$  induced by the flow  $x \in \Omega \mapsto \Phi(x, 0, t)$ , where, given  $0 \leq s \leq t \leq T$ ,  $\Phi(x, s, t)$  denotes the solution of

$$\begin{cases} \dot{x}(r) = b[m](x, r) \quad \forall r \in [s, T], \\ x(s) = x, \end{cases} \quad (8)$$

at time  $t$ , where the trajectory is reflected when it touches the boundary  $\partial\Omega$ .

Given  $M \in \mathbb{N}$ , we construct a mesh on  $\Omega$  defined by a set of vertices  $\mathcal{G}_{\Delta x} = \{x_i \in \Omega, i = 1, \dots, M\}$  and by a set  $\mathcal{T}$  of triangles, whose vertices belong to  $\mathcal{G}_{\Delta x}$  and their maximum diameter is  $\Delta x > 0$ , which form a non-overlapping coverage of  $\Omega$ . We suppose  $\Omega$  to be a polygonal domain, in order to avoid issues related to the approximation of a non-polygonal domain with triangular meshes.

Given  $N \in \mathbb{N}$ , we define the time-step  $\Delta t = T/N$  and consider a uniform partition of  $[0, T]$  given by  $\{t_k = k\Delta t, k = 0, \dots, N-1\}$ .

We consider now a discretization of (7) based on its representation formula by means of the flow  $\Phi$ . For  $\mu \in \mathbb{R}^M$ ,  $j \in \{1, \dots, M\}$ ,  $k = 0, \dots, N-1$ , we define the discrete characteristics as

$$\Phi_{j,k}[\mu] := R(x_j + \Delta t b[\mu](x_j, t_k))$$

where  $R : \mathbb{R}^2 \rightarrow \Omega$  is a reflection operator, related to the Neumann boundary condition, defined as

$$R(z) := \begin{cases} z, & \text{if } z \in \bar{\Omega}, \\ 2 \operatorname{argmin}_{w \in \Omega} |z - w| - z, & \text{if } z \notin \bar{\Omega}. \end{cases}$$

We call  $\{\beta_i ; i = 1, \dots, M\}$  the set of affine shape functions associated to the triangular mesh, such that  $\beta_i(x_j) = \delta_{i,j}$  (the Kronecker symbol) and  $\sum_i \beta_i(x) = 1$  for each  $x \in \bar{\Omega}$ . We define the *median dual control volume* (see Quarteroni (2014) and Voller (2009) for a detailed discussion on the construction of control volumes) by

$$E_i := \bigcup_{T \in \mathcal{T} : x_i \in \partial T} E_{i,T}, \quad \forall i = 1, \dots, M, \quad (9)$$

where  $E_{i,T} := \{x \in T : \beta_j(x) \leq \beta_i(x) \quad j \neq i\}$ .

We approximate the solution  $m$  of the problem (7) by a sequence  $\{m_k\}_k$ , where for each  $k = 0, \dots, N$   $m_k : \mathcal{G}_{\Delta x} \rightarrow \mathbb{R}$  and for each  $i = 1, \dots, M$ ,  $m_{i,k}$  approximates

$$\frac{1}{|E_i|} \int_{E_i} m(x, t_k) dx,$$

where  $|E_i|$  denotes the area of  $E_i$ . We compute the sequence  $\{m_k\}_k$  by the following explicit scheme:

$$m_{i,k+1} = G(m_k, i, k) \quad \forall k = 0, \dots, N-1, \quad i = 1, \dots, M,$$

$$m_{i,0} = \frac{\int_{E_i} m_0(x) dx}{|E_i|} \quad \forall i = 1, \dots, M, \quad (10)$$

where  $G$  is defined by

$$G(w, i, k) := \sum_{j=1}^M \beta_i(\Phi_{j,k}[w]) w_j \frac{|E_j|}{|E_i|},$$

for every  $w \in \mathbb{R}^M$ .

*Remark 2.1.* In the case of a uniform standard quadrilateral mesh, the volume  $E_i$  is given by  $E_i = [x_i^1 - \frac{1}{2}\Delta x, x_i^1 + \frac{1}{2}\Delta x] \times [x_i^2 - \frac{1}{2}\Delta x, x_i^2 + \frac{1}{2}\Delta x]$ ,  $|E_i| = (\Delta x)^2$  for each  $i$  and  $\{\beta_i\}$  represents the  $\mathbb{Q}_1$  basis function associated to the grid.

### 2.3 Fast-marching semi-Lagrangian scheme for the eikonal equation

In order to compute  $\nabla u[m](x, t)$  we need to solve at each time  $t$  an eikonal type equation. For this kind of equations, well known and efficient techniques are Fast Marching Methods (FMM) (Sethian (1999)). These methods have been proposed to speed up the computation of an iterative scheme based on an upwind finite difference discretization of the eikonal equation: the advantage is to have a complexity  $O(M \log(\sqrt{M}))$  with respect to a complexity  $O(M^2)$  of the iterative scheme. The FMM is a one-pass algorithm: the main idea behind it is that the approximation of the solution on the grid is computed following the directions given by the characteristics equations governing the eikonal equation. This ordering allows to compute the approximated solution in only one iteration.

In the context of semi-Lagrangian schemes, a SL version of the FMM scheme for eikonal equations has been proposed in Cristiani and Falcone (2007), moreover a SL version of the FMM scheme on unstructured grid has been proposed in Sethian and Vladimirsky (2001) and Carlini et al. (2013).

## 3. CONGESTION MODELING

The design of the function  $f$  is a delicate matter that deserves a special attention. First of all we notice that the original model (1) is equivalent with the following system (cf. Section 2.1) with the boundary conditions (2):

$$\begin{cases} \partial_t m(x, t) - \operatorname{div}(b[m](x, t) m(x, t)) = 0, \\ b[m](x, t) := f(m(x, t)) \frac{\nabla u(x, t)}{|\nabla u(x, t)|} \\ |\nabla u(x, t)| = \frac{1}{f(m(x, t))}. \end{cases}$$

This system has the positive feature to avoid the numerically difficult computation of the vector field  $f^2(m)\nabla u$ , that, in the congested areas, is the multiplication between two quantities possibly very small  $f^2(m)$  and very big (the modulus of  $\nabla u$ ). Moreover, this formulation clarifies the role of  $f$  as quantifier of the local relation between the speed of the crowd and density. It has been proved experimentally (see e.g. Seyfried et al. (2006); Chattaraj et al. (2009) and Narang et al. (2015)) that this relation

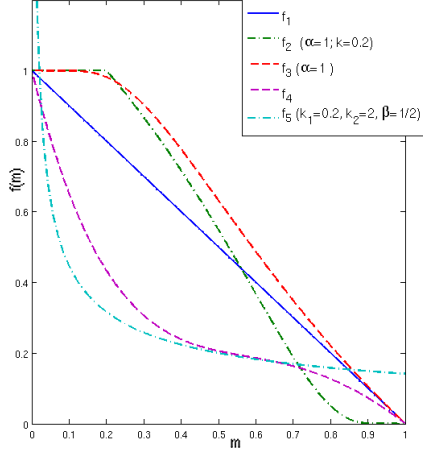


Fig. 1. Fundamental diagrams. For  $f_4$  the coefficients are given by  $a_4 = 112/51$ ,  $a_3 = 380/51$ ,  $a_2 = 434/51$ ,  $a_1 = 213/51$  and  $a_0 = 1$ .

can vary as a function of several physiological and psychological factors such as the state of stress, the knowledge of the environment, etc. The graph of local density/speed is generally called *fundamental diagram*, in analogy with the terminology of vehicular traffic literature. Some examples of well established choices for the diagram are:

$$f_1(m) := 1 - m,$$

$$f_2(m) := \min \left( 1, \exp \left( -\alpha \frac{m - k}{1 - m} \right) \right), \quad \alpha > 0, \quad k \in (0, 1),$$

$$f_3(m) := 1 - \exp \left( -\alpha \frac{1 - m}{m} \right), \quad \alpha > 0,$$

$$f_4(m) := a_4 m^4 - a_3 m^3 + a_2 m^2 - a_1 m + a_0.$$

The choice  $f_1$  appears in Hurley et al. (2015);  $f_3$  has been proposed in the early work by Weidmann (1992) and  $f_2$  can be considered as a variation of it. The diagram  $f_4$  has been proposed and experimentally discussed in Predtechenskii and Milinskii (1978), where the authors proposed the choice of the coefficients reported in the caption of Figure 1. In those models, the maximal speed is scaled by  $1.34 \text{ms}^{-1}$ , which is typically the observed maximal speed of the pedestrians; in the same way, the maximal density before congestion (a value around  $5.4 \text{m}^{-2}$ ) is scaled to 1. Another diagram proposed by Lions (2007-2011), in order to model congestion in Mean Field Games, is given by

$$f_5(m) := \frac{k_1}{(k_2 m)^\beta}, \quad \text{with } 0 < \beta < 1/2, \text{ and } k_1, k_2 > 0.$$

In Figure 1 we present some examples of the various diagrams for some adequate choices of the coefficients. We remark that the diagram of  $f_5$  in Fig. 1 differs strongly from the others, since is not bounded when  $m = 0$  and is not 0 when  $m = 1$ , which means that complete congestion is not allowed.

The effectiveness of an approximation scheme for the system with the diagrams in Fig. 1 is not obvious, since the model requires a very accurate approximation close to the set  $\{(x, t) \in \bar{\Omega} \mid m(x, t) = 1\}$  (congestion). This brings several numerical difficulties that should be addressed in the resolution.

To the best of our knowledge, an organic comparison of

different choices of fundamental diagrams in the Hughes model has never appeared in literature.

#### 4. NUMERICAL SIMULATIONS

In this section we investigate numerically the influence of the penalty function  $f$  in (1). In order to limit instability issues in the congested zones, in the simulations we truncate  $f$ . Given  $\delta > 0$ , in the simulations we replace  $f$  by  $f^\delta$  defined by

$$f^\delta(m) := \max(\delta, f(m)), \quad \text{with } \delta \in \mathbb{R}_+.$$
 (11)

Using the notations in Section 2, we compute the solution of the approximation of (1) iteratively in the following way: given the discrete measure  $m_k$  at time  $t_k$  ( $k = 0, \dots, N - 1$ ), we compute an approximation of the value function  $u(\cdot, t_k)$  using the FMM scheme and the values of  $m_{i,k}$  ( $i = 1, \dots, M$ ). This allows us to construct an approximation  $\nabla u_{i,k}$  of  $\nabla u[m](x_i, t_k)$ . Then, for all  $i = 1, \dots, M$ , we approximate  $b[m](x_i, t_k)$  by  $f(m_{i,k}) \frac{\nabla u_{i,k}}{|\nabla u_{i,k}|}$  and we compute  $m_{\cdot, k+1}$  using (10).

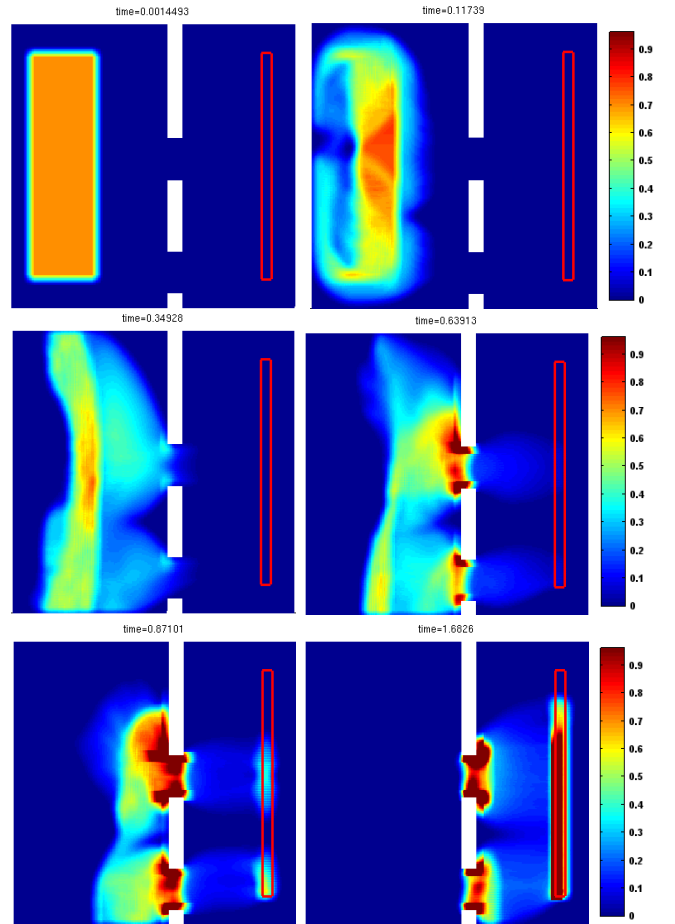


Fig. 2. Evolution of the density with  $f_1$ . The red rectangle is the target region.

In the following simulations we fix

$$\delta = 10^{-3}, \quad \Delta x = 0.0077 \quad \text{and} \quad \Delta t = \Delta x/3.$$

We consider a fix scenario in a domain  $\Omega := ([0, 1] \times [0, 1]) \setminus \Gamma$ , where  $\Gamma := \Gamma_1 \cup \Gamma_2 \cup \Gamma_3$  with

$$\Gamma_1 := [0.55, 0.6] \times [0, 0.05], \quad \Gamma_2 := [0.55, 0.6] \times [0.2, 0.45],$$

$$\Gamma_3 := [0.55, 0.6] \times [0.6, 1].$$

We also fix an initial distribution given by

$$m_0(x) := \begin{cases} 0.7 & x \in [0.1, 0.3] \times [0.1, 0.9], \\ 0 & \text{otherwise,} \end{cases}$$

and a target set  $\mathcal{T} := [0.88, 0.92] \times [0.1, 0.95]$ .

In the first test we choose  $f = f_1$ , which corresponds to a linear penalization of the congestion. This is the most popular choice, see e.g. the original paper by Hughes (2000) and the subsequent works by Di Francesco et al. (2011) and by Carlini et al. (2016). In Figure 2 we observe some of the basic features of the system. The mass, initially given by  $m_0$ , evolves in the direction of the target avoiding the high congested areas (top/left). For this reason the agents initially located on the extreme left hand side of the domain circumvent the center of the domain opting for less crowded regions (top/right). The density moves towards the “doors” and the distribution of the agents takes the typical cone shape observed experimentally in the work by Van den Berg (2009). Then, the crowd splits into two groups crossing the two doors. It is also possible to see (center/left-right) as part of the mass, initially choosing the central door, changes its strategy, preferring the bottom one, which is less congested. We observe that the most congested areas of the narrow passage are in contact with the walls. Note that the crowd remains congested after crossing the doors (bottom/left-right). This peculiar effect is due to the lack of alternative targets and, as we will see, the choice of the model of congestion.

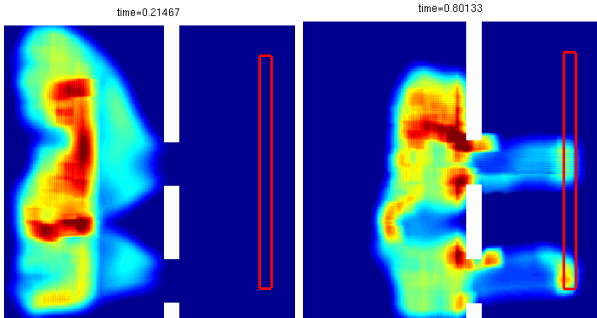


Fig. 3. Evolution of the density with  $f_2$ . The red rectangle is the target region.

For the same initial scenario we consider now the remaining penalty functions. In Figure 3 we display two time instants of the evolution of the system with  $f = f_2$ , the parameters being set as  $\alpha = 1$  and  $k = 0.2$ . In this case, the behaviour of the crowd maintains some features of the previous test, however we can observe an important difference: the maximum value reached by the density is around 0.8 and not 1 as in the previous case. This reflects the fact that, from the perspective of the cost of each microscopic agent, the compromise between the choices of going directly to the target and avoiding congestion (less favorable here) is different than in the previous case.

Now, we choose  $f_3$  with  $\alpha = 1$  as penalty function. In this case, we observe a macroscopic behaviour that mixes some of the features observed so far. As before the crowd splits into two groups associated to each door and we have that a part of the crowd change their strategies, taking into account the congestion. In this case, we observe less congestion of the crowd after crossing the doors. This is

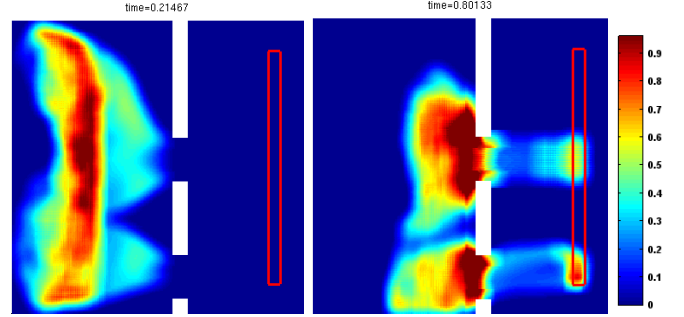


Fig. 4. Evolution of the density with  $f_3$ . The red rectangle is the target region.

possibly due to a higher speed of the agents in the less crowded regions of the domain as imposed by  $f_3$ .

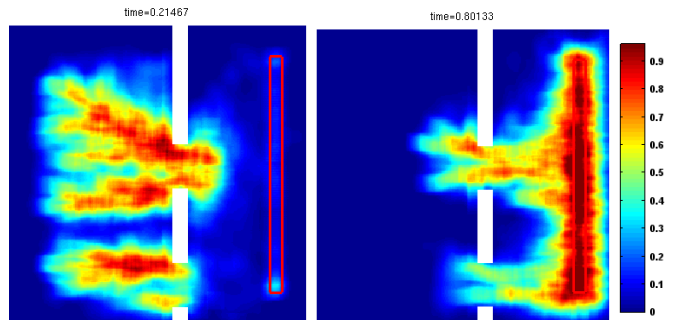


Fig. 5. Evolution of the density with  $f_4$ . The red rectangle is the target region.

With the choice of  $f = f_4$  we observe a very different behavior. In fact  $f_4$  penalizes more the congested regions and it is more suitable to describe ‘nervous’ or ‘panicked’ pedestrians (Predtechenskii and Milinskiĭ (1978)). As a consequence, we do not observe regions of high density and the trajectories chosen by the agents result to be more “chaotic”. In general, as consequence of the choice of the parameters, the time necessary to reach the target for entire crowd is shorter than the ones observed before.

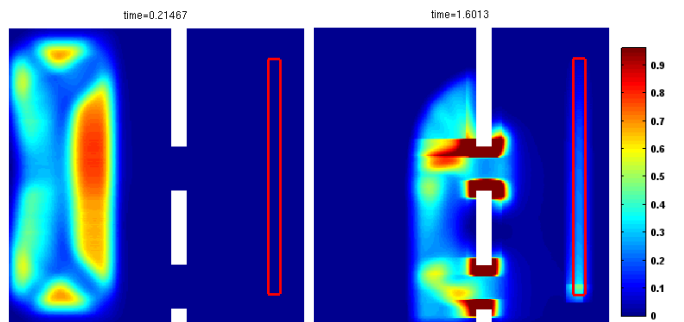


Fig. 6. Evolution of the density with  $f_5$ . The red rectangle is the target region.

The last choice corresponds to  $f = f_5$ . Here, we observe a different splitting. A small part of the crowd, moving at a quite high speed, reaches the target area in a short time. The rest of the crowd concentrates near the doors, increasing the total time to reach the target.

## 5. CONCLUSIONS

In this paper we have considered a SL scheme to solve numerically the first-order Hughes system (1) in the presence of various choices of the fundamental diagram  $f$ . The popularity of such model justifies the study of efficient and stable numerical methods for their resolution. However, many questions are still open. First of all the well-posedness of (1), and its relation with the penalty function  $f$ , is not understood in the two-dimensional case. From the numerical point of view our approach requires some further work. In particular, in view of the lack of theoretical results for the continuous system (1), a convergence theory for our scheme remains still as a difficult challenge.

## REFERENCES

- Amadori, D. and Di Francesco, M. (2012). The one-dimensional Hughes model for pedestrian flow: Riemann-type solutions. *Acta Mathematica Scientia*, 32(1), 259–280.
- Amadori, D., Goatin, P., and Rosini, M.D. (2014). Existence results for Hughes’ model for pedestrian flows. *Journal of Mathematical Analysis and Applications*, 420(1), 387–406.
- Bardi, M. and Dolcetta, I.C. (1996). *Optimal control and viscosity solutions of Hamilton-Jacobi-Bellman equations*. Birkhäuser.
- Bellomo, N. and Dogbe, C. (2011). On the modeling of traffic and crowds: A survey of models, speculations, and perspectives. *SIAM review*, 53(3), 409–463.
- Carlini, E., Falcone, M., and Hoch, P. (2013). A generalized fast marching method on unstructured triangular meshes. *SIAM J. Numer. Anal.*, 51(6), 2999–3035.
- Carlini, E., Festa, A., Silva, F.J., and Wolfram, M.T. (2016). A semi-Lagrangian scheme for a modified version of the Hughes’ model for pedestrian flow. *Dynamic Games and Applications*, 1–23.
- Carlini, E. and Silva, F.J. (2015). A semi-Lagrangian scheme for a degenerate second order mean field game system. *Discrete Contin. Dyn. Syst.*, 35(9), 4269–4292.
- Carlini, E. and Silva, F.J. (2014). A fully discrete semi-Lagrangian scheme for a first order mean field game problem. *SIAM Journal on Numerical Analysis*, 52(1), 45–67.
- Chattaraj, U., Seyfried, A., and Chakroborty, P. (2009). Comparison of pedestrian fundamental diagram across cultures. *Advances in complex systems*, 12(03), 393–405.
- Cristiani, E. and Falcone, M. (2007). Fast semi-Lagrangian schemes for the eikonal equation and applications. *SIAM J. Numer. Anal.*, 45(5), 1979–2011 (electronic).
- Cristiani, E., Piccoli, B., and Tosin, A. (2014). *Multiscale modeling of pedestrian dynamics*, volume 12. Springer.
- Di Francesco, M., Markowich, P.A., Pietschmann, J.F., and Wolfram, M.T. (2011). On the Hughes’ model for pedestrian flow: The one-dimensional case. *Journal of Differential Equations*, 250(3), 1334–1362.
- Festa, A., Tosin, A., and Wolfram, M.T. (2016). Kinetic description of collision avoidance in pedestrian crowds by sidestepping. *ArXiv:1610.05056*, 1–27.
- Hughes, R. (2000). The flow of large crowds of pedestrians. *Mathematics and Computers in Simulation*, 53(4), 367–370.
- Hurley, M.J., Gottuk, D.T., Hall Jr, J.R., Harada, K., Kuligowski, E.D., Puchovsky, M., Watts Jr, J.M., Wieczorek, C.J., et al. (2015). *SFPE Handbook of fire protection engineering*. Springer.
- Lions, P.L. (2007-2011). Cours du collège de France.
- Narang, S., Best, A., Curtis, S., and Manocha, D. (2015). Generating pedestrian trajectories consistent with the fundamental diagram based on physiological and psychological factors. *PLoS one*, 10(4), e0117856.
- Piccoli, B. and Tosin, A. (2011). Time-evolving measures and macroscopic modeling of pedestrian flow. *Archive for Rational Mechanics and Analysis*, 199(3), 707–738.
- Predtechenskii, V. and Milinskiĭ, A.I. (1978). *Planning for foot traffic flow in buildings*. NBS, US Department of Commerce, and the NSF, Washington, DC.
- Quarteroni, A. (2014). *Numerical models for differential problems*, volume 8 of *MS&A. Modeling, Simulation and Applications*. Springer, Milan, second edition. Translated from the fifth (2012) Italian edition by Silvia Quarteroni.
- Sethian, J.A. (1999). Fast marching methods. *SIAM Rev.*, 41(2), 199–235.
- Sethian, J.A. and Vladimirsky, A. (2001). Ordered upwind methods for static Hamilton-Jacobi equations. *Proc. Natl. Acad. Sci. USA*, 98(20), 11069–11074.
- Seyfried, A., Steffen, B., and Lippert, T. (2006). Basics of modelling the pedestrian flow. *Physica A: Statistical Mechanics and its Applications*, 368(1), 232–238.
- Van den Berg, M. (2009). *Pedestrian behaviour and its relation to doorway capacity*. Ph.D. thesis, TU Delft, Delft University of Technology.
- Voller, V.R. (2009). *Basic control volume finite element methods for fluids and solids*, volume 1 of *IISc Research Monographs Series*. World Scientific Publishing Co. Pte. Ltd., Hackensack, NJ; IISc Press, Bangalore.
- Weidmann, U. (1992). *Transporttechnik der fussgänger*. IVT, Institut für Verkehrsplanung, Transporttechnik, Strassen-und Eisenbahnbau.